Modelling vaporous cavitation on fluid transients

Shu, Jian Jun

2003

https://hdl.handle.net/10356/93924

https://doi.org/10.1016/S0308-0161(03)00025-5

Modelling vaporous cavitation on fluid transients

Jian-Jun Shu

School of Mechanical and Production Engineering, Nanyang Technological University,
50 Nanyang Avenue, Singapore, Singapore 639798
Tel.: +65-6790-4459; fax: +65-6791-1859.
E-mail address: mjjshu@ntu.edu.sg (J.-J. Shu).

Abstract

A comprehensive study of the problem of modelling *vaporous cavitation* in transmission lines is presented. The *two-phase homogeneous equilibrium vaporous cavitation model* which has been developed is compared with the conventional *column separation model*. The latter predicts unrealistically high pressure spikes because of a conflict arising from the prediction of negative cavity sizes if the pressure is not permitted to fall below the vapour pressure, or the prediction of negative absolute pressures if the cavity size remains positive. This is verified by a comparison of predictions with previously published experimental results on upstream, midstream and downstream cavitation. The new model has been extended to include frequency-dependent friction. The characteristics predicted by the *frequency-dependent friction model* show close correspondence with experimental data.

Keywords: Vaporous cavitation; Fluid transients; Transmission lines; Column separation; Frequency-dependent friction

1. Introduction

In hydraulic systems, cavitation can have a serious effect upon the performance of pumps, valves and other components. For the case of positive displacement pumps, the collapse of cavitation bubbles may cause surface damage to the pump and to other components as the surface debris is carried through the system by the working fluid. Severe cavitation reduces volumetric efficiency. Consequently, in order to improve the performance and reliability of systems, it is important to be able to predict the onset and degree of cavitation taking place. This will enable improvements to be made to both pump and circuit design.

Fluid mixtures in hydraulic systems can be classified into five states according to the working conditions: (1) fully degassed liquid; (2) fully degassed liquid with vapour; (3) liquid with dissolved gas; (4) liquid with dissolved and undissolved gas and (5) liquid with dissolved gas, undissolved gas and vapour. If we consider a liquid with dissolved gas, then depending upon the magnitude of the pressure reduction which is occurring in the system and its rate of change, gas cavities may initially be formed due to the presence

of suitable nuclei (contaminant, for example). These cavities grow slowly by the diffusion of dissolved gas evolving from the liquid. The process is called *gaseous cavitation* [1,2]. When the pressure falls below the vapour pressure of a liquid, the cavities grow very rapidly because of evaporation into the growing cavity. The process is called *vaporous cavitation* which is, in a sense, a true cavitation. At present the general approach in transmission line modelling is to assume column separation (see, for example, Wylie and Streeter [3,4], Simpson and Wylie [5] and Bergant and Simpson [6]). However, such an approach is over-simplistic and can lead to unrealistic predictions. In this paper a brief review of the classical approach to vaporous cavitation is presented and followed by the development of an improved model. When vaporous cavities are locally incipient or desinent, the local pressures may be less than or greater than the vapour pressure of the liquid. However, for modelling purposes in engineering, it is assumed that the local pressures are equal to the vapour pressure when vaporous cavitation is taking place.

2. Column separation

For the cases where the dissolved content of a liquid is low (for example, water at atmospheric pressure and 25 ℃ contains 1.84% dissolved air by volume) cavities are primarily in the form of vaporous cavitation when the vapour pressure of the liquid is reached.

An early attempt to evaluate the effect of vaporous cavitation has been described by Siemons [7], followed by Baltzer [8]. Both assumed that in the top part of a horizontal tube, a thin cavity develops containing vapour at a constant vapour pressure. The flow underneath can be considered incompressible, which enables a mathematical model to be established. The results do not have general validity because the test case is arbitrary.

Without focusing on the bubble dynamics of two-phase flow, Wylie and Streeter [3,4] divided a tube into N equal elements, each Δx in length as shown in Fig. 1. The vaporous cavities are assumed to be concentrated at fixed computing nodes and no cavities exist within each element. The one-dimensional equations of continuity and momentum are

$$\frac{1}{c_0^2}\frac{\partial P}{\partial t} + \frac{\rho_l}{\pi r_0^2}\frac{\partial Q}{\partial x} = 0, \tag{1}$$

$$\frac{\rho_l}{\pi r_0^2}\frac{\partial Q}{\partial t} + \frac{\partial P}{\partial x} + F_0(Q) + \rho_l g \sin\theta_0 = 0, \tag{2}$$

where P, Q are instantaneous pressure and volumetric flow rate of the liquid, which has liquid density ρ_l; r_0 is the internal radius of tube; θ_0 is the inclination of the tube to the horizontal which is positive when the elevation increases in the $+x$ direction, measured along the tube; c_0 is the speed of sound in the tube:

$$c_0^2 = \frac{K_l}{\rho_l}.$$

When the elasticity of the tube wall is considered, c_0 will be modified as

$$c_0^2 = \frac{K_l/\rho_l}{1 + \dfrac{2\kappa_l r_0}{Ee}},$$

where K_l, E and e are bulk modulus of elasticity of the liquid, Young's modulus and thickness of the tube, respectively.

For laminar flow, the viscous loss term $F_0(Q)$ can be expressed in terms of the one-dimensional linear resistance compressible flow model [9–12], or the 'exact' first-order model [13–19], or other distributed parameter approaches [20,21]; For turbulent flow, a model with the Darcy-Weisbach friction factor f [3,4] is used

$$F_0(Q) = \frac{f\rho_l Q|Q|}{4\pi^2 r_0^5}. \tag{3}$$

Using the method of characteristics, two finite-difference equations are expressed as

$$C^+: \frac{\rho_l}{\pi r_0^2}Q_D + \frac{1}{c_0}P_D = C_A, \tag{4}$$

$$C^-: \frac{\rho_l}{\pi r_0^2}Q_D - \frac{1}{c_0}P_D = C_B, \tag{5}$$

in which C_A and C_B are always known constants when the equations are applied:

$$C_A = \frac{\rho_l}{\pi r_0^2}Q_A + \frac{1}{c_0}P_A - \frac{\Delta x}{c_0}F_0(Q_A) - \frac{\rho_l g \Delta x}{c_0}\sin\theta_0, \tag{6}$$

$$C_B = \frac{\rho_l}{\pi r_0^2}Q_B - \frac{1}{c_0}P_B - \frac{\Delta x}{c_0}F_0(Q_B) - \frac{\rho_l g \Delta x}{c_0}\sin\theta_0. \tag{7}$$

Ignoring mass transfer during cavitation, a continuity equation for the vapour volume V is applied at each computing node

$$\frac{\partial V}{\partial t} = Q_2 - Q_1. \tag{8}$$

Two subscripts 1 and 2 are used to indicate left and right limits at each computing node. The resultant finite-difference equation is

$$V_D = V_E + \frac{\Delta x}{2c_0}\left(Q_{D_2} - Q_{D_1} + Q_{E_2} - Q_{E_1}\right). \tag{9}$$

This model is based on the *column separation* hypothesis that the flow of liquid in the tube is instantaneously and completely separated by its vapour phase when the cavity is formed. For the magnitudes of the transient pressures and velocities ordinarily encountered with viscous flow in a horizontal or near-horizontal tube terminated by a valve, the column separation hypothesis does not imply complete physical interruption of the flowing liquid. In fact, once development of a cavity has occurred at some point in the

pipe, the cavity usually expands and propagates in the direction of flow as an elongated bubble. So column separation does not necessarily occur in practice, especially in a horizontal or near-horizontal tube.

During the existence of the cavity, an internal boundary condition is established in the *vapour column separation model* at each computing node. A computer program chart to solve the problem of vaporous cavitation is presented by Wylie and Streeter [3,4] and is summarized in Appendix A.

3. Two-phase homogeneous equilibrium vaporous cavitation

Although the vapour column separation model is easily implemented and faithfully reproduces many of the essential features of a physical event, it has some serious deficiencies:

(i) To avoid the prediction of a negative cavity size (if the pressure is not permitted to fall below the vapour pressure), or the prediction of negative absolute pressures (if the cavity size remains positive), artificial restrictions are imposed (see Fig. 2 and the Steps 7 and 9 in Appendix A). These result in unrealistically large pressure spikes that discredit the overall value of the numerical results.

(ii) The internal boundary condition (9) permits, subjectively, vapour cavities to be formed only at computing nodes. The simulation results are strongly biased according to where the computing nodes are located.

(iii) Because the size of the cavity and its mass transfer are ignored at each computing node, this model is clearly limited in its ability to model cavitation correctly.

(iv) At each computing node, a flow rate discontinuity is assumed. Hence, for a given location in the pipe, there will be two predicted values of flow rate, which is clearly inconsistent with the true (measured) behaviour at this point. In addition, the difference between the two predicted values increases when there is a high degree of cavitation and also when the number of computing nodes is small. However, when a large number of computing nodes is used, there are a corresponding number of discontinuities leading to a mathematical model that is ill defined.

When the pressure falls to the vapour pressure of the liquid during transient flows, vaporization occurs. Vapour cavities may be physically dispersed homogeneously (bubbles evenly distributed), or collected into a single or multiple void space, or a combination of the two. The behaviour can be described by two-phase flow theory. Single-phase flow becomes a special case when no vaporization occurs. In this section a *two-phase homogeneous equilibrium vaporous cavitation model* is presented as an alternative formulation to overcome the above deficiencies and improve the reliability of numerical modelling of vaporous cavitation.

A difference in velocity between the liquid phase and vapour phase will promote mutual momentum transfer. Often these processes proceed very rapidly and it can be assumed that equilibrium conditions prevail. In other words, a vapour cavity shares the same velocity and pressure as the liquid flow at the point where vaporous cavitation

occurs. The average values of velocity in the two-phase mixture are the same as the values for each phase and, in this paper, the author proposes a mathematical model named *homogeneous equilibrium flow model*.

The basic equations for the unsteady homogeneous equilibrium flow model in a tube are:

$$\frac{1}{c_0^2}\frac{\partial P}{\partial t} + (\rho_l - \rho_v)\frac{\partial \alpha}{\partial t} + \frac{\rho_m}{\pi r_0^2}\frac{\partial}{\partial x}\left(\frac{Q}{\alpha}\right) = 0, \qquad (10)$$

$$\frac{\rho_m}{\pi r_0^2}\frac{\partial}{\partial t}\left(\frac{Q}{\alpha}\right) + \frac{\partial P}{\partial x} + F_0\left(\frac{Q}{\alpha}, \alpha\right) + \rho_m g \sin \theta_0 = 0. \qquad (11)$$

In terms of the volumetric fraction α of liquid and vapour phase density ρ_v; the mean density ρ_m can be expressed in

$$\rho_m = \alpha\rho_l + (1 - \alpha)\rho_v.$$

In the above equations the second term in Eq. (10) describes the interfacial mass transfer rate and the term Q/α in Eqs. (10) and (11) indicates the difference between the liquid phase flowrate and the vapour phase flowrate. Using the Darcy-Weisbach friction factor f; the term $F_0(Q/\alpha, \alpha)$ can be expressed as

$$F_0\left(\frac{Q}{\alpha}, \alpha\right) = \frac{f\rho_m Q|Q|}{4\pi^2\alpha^2 r_0^5}. \qquad (12)$$

The method of characteristics is used to transform the above equations to four ordinary differential equations

$$C^+ : \begin{cases} \dfrac{1}{\pi r_0^2}\dfrac{d}{dt}\left(\dfrac{Q}{\alpha}\right) + \dfrac{1}{\rho_l c_0}\dfrac{d}{dt}(P - p_v) + c_0\dfrac{\partial}{\partial t}\left(\ln\dfrac{\rho_m}{\rho_l}\right) \\[2mm] \qquad\qquad + \dfrac{fQ|Q|}{4\pi^2\alpha^2 r_0^5} + g \sin \theta_0 = 0, \\[3mm] \dfrac{dx}{dt} = c_0, \end{cases}$$

$$C^- : \begin{cases} \dfrac{1}{\pi r_0^2}\dfrac{D}{Dt}\left(\dfrac{Q}{\alpha}\right) - \dfrac{1}{\rho_l c_0}\dfrac{D}{Dt}(P - p_v) - c_0\dfrac{\partial}{\partial t}\left(\ln\dfrac{\rho_m}{\rho_l}\right) \\[2mm] \qquad\qquad + \dfrac{fQ|Q|}{4\pi^2\alpha^2 r_0^5} + g \sin \theta_0 = 0, \\[3mm] \dfrac{Dx}{Dt} = -c_0. \end{cases}$$

The equations needed to solve for the variables at each time step are:

$$C^+ : \frac{1}{\pi r_0^2}\frac{Q_D}{\alpha_D} + \frac{1}{\rho_l c_0}(P_D - p_v) + \frac{c_0}{2}\ln\frac{\rho_{m_D}}{\rho_l} = C_A, \qquad (13)$$

$$C^- : \frac{1}{\pi r_0^2}\frac{Q_D}{\alpha_D} - \frac{1}{\rho_l c_0}(P_D - p_v) - \frac{c_0}{2}\ln\frac{\rho_{m_D}}{\rho_l} = C_B. \qquad (14)$$

By solving for Q_D, P_D and $\alpha_D = (\rho_{m_D} - \rho_v)/(\rho_1 - \rho_v)$, C_A and C_B are known constants when the equations are applied:

$$C_A = \frac{1}{\pi r_0^2}\frac{Q_A}{\alpha_A} + \frac{1}{\rho_l c_0}(P_A - p_v) + \frac{c_0}{2}\ln\frac{\rho_{m_E}\rho_{m_F}}{\rho_l\rho_{m_A}}$$

$$\qquad - \frac{f\Delta x Q_A|Q_A|}{4\pi^2\alpha_A^2 r_0^5 c_0} - \frac{g\Delta x}{c_0}\sin\theta_0, \qquad (15)$$

$$C_B = \frac{1}{\pi r_0^2}\frac{Q_B}{\alpha_B} - \frac{1}{\rho_l c_0}(P_B - p_v) - \frac{c_0}{2}\ln\frac{\rho_{m_E}\rho_{m_G}}{\rho_l\rho_{m_B}}$$

$$\qquad - \frac{f\Delta x Q_B|Q_B|}{4\pi^2\alpha_B^2 r_0^5 c_0} - \frac{g\Delta x}{c_0}\sin\theta_0. \qquad (16)$$

Unlike the vapour column separation model, no conflict between negative cavity sizes and pressures below the vapour pressure is introduced

if $C_A \geq C_B$, then $\alpha_D = 1$, $P_D = \frac{\rho_l c_0}{2}(C_A - C_B) + p_v$, $\qquad (17)$

if $C_A < C_B$, then $P_D = p_v$,

$$\alpha_D = \frac{\rho_l \exp\dfrac{C_A - C_B}{c_0} - p_v}{\rho_1 - \rho_v}. \qquad (18)$$

In either case,

$$Q_D = \frac{\pi r_0^2 \alpha_D}{2}(C_A + C_B). \qquad (19)$$

A computer program chart of the two-phase homogeneous equilibrium vaporous cavitation model is given in Appendix B. This is readily implemented and overcomes the major deficiencies of the vapour column separation model.

4. Frequency-dependent friction

It is well known that fluid friction losses are dependent not only upon the average velocity at the instant, but also upon the history of the average velocity in transient flow. This is called *frequency-dependent friction* and results in higher frequencies being attenuated much more rapidly than low frequency components of velocity. The Darcy-Weisbach equation (12) does not account for such effects.

Zielke [22] has developed appropriate friction terms using a weighting function for transient laminar flow, but direct numerical integration of the equations requires a large

amount of calculation. Some efficient procedures have been developed by Trikha [23] and then Kagawa et al. [24]. The procedures consist of approximating the exact Zielke weighting function as a sum of impulse responses of first order lags. Much less computer storage and computation time are two important benefits. The error incurred as a result of the approximation is adjustable using the method posed by Kagawa et al. [24] and is therefore much more accurate than Trikha model. Consequently, in this paper, Kagawa's weighting function will be adopted.

Good progress has been made in developing relations for turbulent flow with frequency-dependent friction by Hirose [25], Margolis and Brown [26], Brown [27,28], Brown and Linney [29], Vardy and Brown [30], and Shu [31]. However, little work appears to have been undertaken on frequency-dependent friction under two-phase flow conditions. Reasoning from an analogy to laminar flow, the author suggests using the following expression for frequency-dependent friction $F(Q/\alpha, \alpha)$ in turbulent, two-phase flow

$$F\left(\frac{Q}{\alpha}, \alpha\right) = F_0\left(\frac{Q}{\alpha}, \alpha\right) + \frac{1}{2}\left(W * \frac{\partial F_0}{\partial t}\right)(t), \qquad (20)$$

where the convolution integral is defined as $(f * g)(t) = \int_0^t f(t - \lambda)g(\lambda)d\lambda$. $F_0(Q/\alpha, \alpha)$ is a steady friction term and $W(t)$ is a weighting function. The foregoing relationship is based upon the following:

(i) The nature of the weighting function is to smooth rapid changes in flow velocity for laminar flow conditions. Here the author proposes a more general smoothing function that may be applied to laminar, turbulent and multi-phase flow.

(ii) Viscosity effects are not well defined in turbulent two-phase flows. No viscosity appears explicitly in the relationship (20).

(iii) The well-defined case of transient laminar flow is inclusive.

(iv) The relationship has sufficient generality that the weighting function can be designed by some given criteria depending on the application; the manner is analogous to smoothing filter design in signal processing.

The steady-state friction value $F_0(Q/\alpha, \alpha)$ is the same as (12)

$$F_0\left(\frac{Q}{\alpha}, \alpha\right) = \frac{f\rho_m Q|Q|}{4\pi^2 \alpha^2 r_0^5}. \qquad (21)$$

The weighting function $W(t)$ can be approximated by sum of k impulse responses of first order elements

$$W(t) = \sum_{i=1}^{k} m_i E^{-n_i \tau}, \qquad (22)$$

where m_i and n_i can be determined by curve fitting [24] to the Zielke weighting function as listed in Table 1. The parameter $\tau = \mu_m t / \rho_m r_0^2$ is a non-dimensional delay time and the 'virtual' viscosity μ_m for the two-phase mixture is expressed by Dukler's expression [32,33] in terms of liquid viscosity μ_l and vapour viscosity μ_v

$$\mu_m = \alpha\mu_l + (1 - \alpha)\mu_v. \tag{23}$$

A simple recursive form for $F(Q/\alpha, \alpha)$ in Eq. (20) has been developed by Kagawa et al. [24] that only requires characteristic data from the last time step.

$$F|_{t+\Delta t} = F_0|_{t+\Delta t} + \frac{1}{2}\sum_{i=1}^{k} y_i(t + \Delta t) \tag{24}$$

with

$$\begin{cases} y_i(t + \Delta t) = y_i(t)e^{-n_i\Delta\tau} + m_i e^{-n_i(\Delta\tau/2)}[F_0|_{t+\Delta t} - F_0|_t], \\ y_i(0) = 0, \end{cases} \tag{25}$$

where

$$\Delta\tau = \frac{\Delta t}{r_0^2}\frac{\mu_m}{\rho_m}\bigg|_{t+(\Delta t/2)}. \tag{26}$$

From Eq. (25), it is evident that a good approximation to $W(t)$ over a region of $\tau > \Delta\tau/2$ makes the numerical integration approach presented by Zielke accurate. In Table 1, τ_{m_i} is such τ that the relative error between $W(t)$ and the Zielke weighting function [22] becomes less than 1% over a region of $\tau > \tau_{m_i}$ and for a calculation error of less than 1%, k is determined according to $\Delta\tau/2 > \tau_{m_i}$. Using the characteristics method for Eqs. (10) and (11) together with characteristics Eqs. (13) and (14), the following is obtained

$$\Delta\tau_A = \frac{\Delta x}{2r_0^2 c_0}\left(\frac{\mu_{m_A}}{\rho_{m_A}} + \frac{\mu_{m_F}}{\rho_{m_F}}\right),$$

$$\Delta\tau_B = \frac{\Delta x}{2r_0^2 c_0}\left(\frac{\mu_{m_B}}{\rho_{m_B}} + \frac{\mu_{m_G}}{\rho_{m_G}}\right), \tag{27}$$

and

$$F_A = \frac{f\rho_{m_A}Q_A|Q_A|}{4\pi^2\alpha_A^2 r_0^5} + \frac{1}{2}\sum_{i=1}^{k}\left[y_{i_A}e^{-n_i\Delta\tau_A} + \frac{fm_i}{4\pi^2 r_0^5}e^{-n_i(\Delta\tau_A/2)}\right.$$
$$\left. \times\left(\frac{\rho_{m_A}Q_A|Q_A|}{\alpha_A^2} - \frac{\rho_{m_F}Q_F|Q_F|}{\alpha_F^2}\right)\right]. \tag{28}$$

$$F_B = \frac{f \rho_{m_B} Q_B |Q_B|}{4\pi^2 \alpha_B^2 r_0^5} + \frac{1}{2} \sum_{i=1}^{k} \left[y_{i_B} e^{-n_i \Delta \tau_B} + \frac{f m_i}{4\pi^2 r_0^5} e^{-n_i (\Delta \tau_B / 2)} \right.$$
$$\left. \times \left(\frac{\rho_{m_B} Q_B |Q_B|}{\alpha_B^2} - \frac{\rho_{m_G} Q_G |Q_G|}{\alpha_G^2} \right) \right], \qquad (29)$$

and

$$C_A = \frac{1}{\pi r_0^2} \frac{Q_A}{\alpha_A} + \frac{1}{\rho_l c_0} (P_A - p_v) + \frac{c_0}{2} \ln \frac{\rho_{m_E} \rho_{m_F}}{\rho_l \rho_{m_A}}$$
$$- \frac{\Delta x F_A}{\rho_{m_A} c_0} - \frac{g \Delta x}{c_0} \sin \theta_0, \qquad (30)$$

$$C_B = \frac{1}{\pi r_0^2} \frac{Q_B}{\alpha_B} - \frac{1}{\rho_l c_0} (P_B - p_v) - \frac{c_0}{2} \ln \frac{\rho_{m_E} \rho_{m_G}}{\rho_l \rho_{m_B}}$$
$$- \frac{\Delta x F_B}{\rho_{m_B} c_0} - \frac{g \Delta x}{c_0} \sin \theta_0. \qquad (31)$$

The computer program chart of the two-phase homogeneous equilibrium vaporous cavitation model with frequency-dependent friction is presented in Appendix C.

5. Experimental verification

Experiments on vaporous cavitation have been conducted by Sanada et al. [34] using a horizontal acrylic pipeline and water as the working fluid. They examined vaporous cavitation which they classified as upstream-, midstream- and downstream-type. The test rig is shown in Fig. 3 and the essential parameters are listed in Table 2.

When an upstream valve is rapidly closed in a flowing liquid line, the pressure at the vicinity of the valve is reduced to the vapour pressure and cavities are formed. After a certain time, a reflected pressure wave will collapse the cavities and possibly cause very high pressures at the valve. Several cycles of cavity formation and collapse occur before frictional effects damp the oscillations sufficiently for the minimum pressure at the valve to remain permanently above the vapour pressure. This is *upstream cavitation*. Hydraulic transients in pump delivery lines induced by pump failure [35–38] result in upstream cavitation.

When the upstream pressure quickly drops down to a certain level in a flowing liquid line, rarefaction waves will be sent downstream. The pressure at some location in the line may be reduced to the vapour pressure and cavities may be formed. The reflected pressure waves and rarefaction waves in the line will have a dominant effect on the behaviour of the cavities. This is *midstream cavitation*. Hydraulic transients in pump delivery lines induced by pump pulsation [39] may result in midstream cavitation.

When the downstream valve is suddenly shut in a flowing liquid line, the liquid will accumulate in the vicinity of the valve. A high pressure at the vicinity of the valve cause flow reversal and several cycles of cavity formation and collapse will consequently occur

as a result of fluid accumulation and dissipation. This is *downstream cavitation*. Hydraulic transients in pump suction lines induced by pump failure [8,40] result in downstream cavitation.

In the experimental studies conducted by Sanada et al. [34] the absolute pressure head, $H = P/\rho_1 g$ was recorded as a function of time at different locations, according to the class of cavitation being investigated.

Fig. 4 shows the measured behaviour together with predictions from the various models for upstream cavitation. For this case, where cavitation is severe, the predictions all show similar characteristics, but the high frequency components superimposed on the waveform are rather better damped when frequency-dependent friction is included; this is closer to the measured response. The superiority of the frequency-dependent friction model is much more apparent for the case of midstream cavitation (Fig. 5) and downstream cavitation (Fig. 6). For both cases, there is good agreement between the frequency-dependent friction model predictions and observed behaviour. This is because the weighting functions in Table 1 correspond to laminar, single-phase flow conditions, which match conditions more closely when cavitation is not too severe.

6. Conclusions

The method of characteristics approach to the modelling of wave transients in fluid transmission lines has been extended to include two-phase flow following vaporous cavitation. The resultant equations ((10), (11) and (20)) predict closely the pressure transients for vaporous cavitation conditions following sudden closure of a valve in a pipeline; the largest errors are encountered when cavitation is severe. The use of the mathematical model (10), (11) and (20) provides a powerful and basic tool to understand the mechanism of transient fluid flow with vaporous cavitation in transmission lines. The modifying weighting function for frequency-dependent friction (20) is a key to producing improved predictions for two-phase transient flows. More work is required to establish appropriate weighting functions particularly for the case of two-phase flow.

Appendix A. Computer program chart for vapour column separation model

Step 1: Calculate initial steady-state conditions for P, Q and V;

Step 2: Increment the time by $\Delta t = \Delta x / c_0$;

Step 3: If $V_E > 0$, go to Step 5;

Step 4: Calculate P_D from both Eqs. (4) and (5) together and if $P_D \geq p_v$ (vapour pressure), go to Step 10;

Step 5: Set $P_D = p_v$ and calculate Q_{D_1} from Eq. (4) and Q_{D_2} from Eq. (5) separately;

Step 6: Calculate V_D from Eq. (9) and if $V_D > 0$, go to Step 11;

Step 7: Set $V_D = 0$ and calculate P_D from both Eqs. (4) and (5) together;

Step 8: If $P_D \geq p_v$, go to Step 10;

Step 9: Set $P_D = p_v$ and $V_D = 0$;

Step 10: Set $V_D = 0$ and calculate $Q_{D_1} = Q_{D_2}$ from both Eqs. (4) and (5) together;

Step 11: Calculate boundary conditions for P, Q and V;

Step 12: Check to see if a given maximum time tolerance has been exceeded. If not, go to Step 2; Otherwise, terminate calculations and print out results.

Appendix B. Computer program chart for two-phase homogeneous equilibrium vaporous cavitation model

Step 1: Calculate initial steady-state conditions for P, Q and α;

Step 2: Increment the time by $\Delta t = \Delta x / c_0$;

Step 3: Calculate C_A from Eq. (15) and C_B from Eq. (16);

Step 4: If $C_A \geq C_B$, set $\alpha_D = 1$ and calculate P_D from Eq. (17);

Step 5: If $C_A < C_B$, set $P_D = p_v$ and calculate α_D from Eq. (18);

Step 6: Calculate Q_D from Eq. (19);

Step 7: Calculate boundary conditions for P, Q and α;

Step 8: Check to see if a given maximum time tolerance has been exceeded. If not, go to Step 2; otherwise terminate the calculations and print out the results.

Appendix C. Computer program chart for two-phase homogeneous equilibrium vaporous cavitation model with frequency-dependent friction

Step 1: Calculate initial steady-state conditions for P, Q and α and set $y_i = 0, 1 \leq i \leq 10$ at each computing node;

Step 2: Increment the time by $\Delta t = \Delta x / c_0$;

Step 3: Calculate $\Delta \tau_A$ and $\Delta \tau_B$ from Eq. (27) and determining k satisfied by $\min(\Delta \tau_A / 2, \Delta \tau_B / 2) > \tau_{m_i}$ from Table 1;

Step 4: Calculate F_A from Eq. (28) and F_B from Eq. (29);

Step 5: Calculate C_A from Eq. (30) and C_B from Eq. (31);

Step 6: If $C_A \geq C_B$, set $\alpha_D = 1$ and calculate P_D from Eq. (17);

Step 7: If $C_A < C_B$, set $P_D = p_v$ and calculate α_D from Eq. (18);

Step 8: Calculate Q_D from Eq. (19);

Step 9: Calculate boundary conditions for P, Q and α;

Step 10: Updating y_i, $1 \leq i \leq 10$ from Eq. (25);

Step 11: Check to see if a given maximum time tolerance has been exceeded. If not, go to Step 2; otherwise, the calculations are terminated and the results are printed out.

References

[1] Wiggert DC, Sundquist MJ. The effect of gaseous cavitation on fluid transients. Trans ASME, J Fluids Engng 1979;101(1):79–86.

[2] Wylie EB. Simulation of vaporous and gaseous cavitation. Trans ASME, J Fluids Engng 1984;106(3):307–11.

[3] Wylie EB, Streeter VL. Fluid transients. New York: McGraw-Hill; 1978.

[4] Wylie EB, Streeter VL. Fluid transients in systems. Englewood Cliffs, NJ: Prentice-Hall; 1993.

[5] Simpson AR, Wylie EB. Large water-hammer pressures for column separation in pipelines. J Hydraul Engng 1991;117(10):1310–6.

[6] Bergant A, Simpson AR. Pipeline column separation flow regimes. J Hydraul Engng 1999;125(8):835–48.

[7] Siemons J. The phenomenon of cavitation in a horizontal pipe-line due to a sudden pump failure. J Hydraul Res 1967;5:135–52.

[8] Baltzer RA. Column separation accompanying liquid transients in pipes. Trans ASME, J Basic Engng 1967;89:837–46.

[9] Constantinesco G. Theory of wave transmission—a treatise on transmission of power by vibrations. London: Walter Haddon; 1922.

[10] Oldenburger R, Goodson RE. Simplification of hydraulic line dynamics by use of infinite products. Trans ASME, J Basic Engng 1964;86:1–10.

[11] Schuder CB, Binder RC. The response of pneumatic transmission lines to step inputs. Trans ASME, J Basic Engng 1959;81:578–84.

[12] Wood FM. The application of heaviside's operational calculus to the solution of problems in water hammer. Trans Jpn Soc Mech Engnr, Ser B 1937;HYD-59-15:707–13.

[13] Cohen H, Tu YO. Viscosity and boundary effects in the dynamic behavior of hydraulic systems. Trans ASME, J Basic Engng 1962;84: 593–601.

[14] Gerlach CR. The dynamics of viscous fluid transmission lines with particular emphasis on higher model propagation. PhD Thesis. Oklahoma State University, USA; 1966.

[15] Gerlach CR, Parker JD. Wave propagation in viscous fluid lines including higher model effects. Trans ASME, J Basic Engng 1967;89: 782–8.

[16] Inaba T, Hashimoto M, Miyake Y, Murata S. Pulsating laminar flow in a cylindrical pipe with through flow. Bull JSME 1977;20(142):442–9.

[17] Ohmi M, Usui T, Fukawa M, Hirasaki S. Pressure and velocity distributions in pulsating laminar pipe flow. Bull JSME 1976;19(129): 298–306.

[18] Scarton HA. Waves and stability in viscous and inviscid compressible liquids contained in rigid and elastic tubes by the method of eigenvalues. PhD Thesis. Carnegie-Mellon University, Pittsburgh, USA; 1970.

[19] Urata E. Unsteady flow of viscous liquid in long circular tube. Bull JSME 1971;14(68):147–55.

[20] Stecki JS, Davis DC. Fluid transmission lines—distributed parameter models. Part 1. A review of the state of the art. Proc Inst Mech Engnr, Part A, Power Process Engng 1986;200(A4):215–28.

[21] Stecki JS, Davis DC. Fluid transmission lines—distributed parameter models. Part 2. Comparison of models. Proc Inst Mech Engnr, Part A, Power Process Engng 1986;200(A4):229–36.

[22] Zielke W. Frequency-dependent friction in transient pipe flow. Trans ASME, J Basic Engng 1968;90:109–15.

[23] Trikha AK. An efficient method for simulating frequency-dependent friction in transient liquid flow. Trans ASME, J Fluids Engng 1975; 97:97–105.

[24] Kagawa T, Lee IY, Kitagawa A, Takenaka T. High speed and accurate computing method of frequency-dependent friction in laminar pipe flow for characteristics method. Trans Jpn Soc Mech Engnr, Ser B 1983;49(447):2638–44. in Japanese.

[25] Hirose M. Frequency-dependent wall shear in transient fluid flow simulation of unsteady turbulent flow. MSc Thesis. Department of Mechanical Engineering, Massachusetts Institute of Technology; 1971.

[26] Margolis DL, Brown FT. Measurement of the propagation of long-wavelength disturbances through turbulent flow in tubes. ASME Paper 75-FE-22 presented at Fluids Engineering Conference, Minneapolis, USA; 1975.

[27] Brown FT. Wave propagation in tubes with turbulent flow. Part I. Analytical models. In: Franke ME, Drzewiecki TM, editors. Proceedings of Symposium on Fluid Transmission Line Dynamics. The Winter Annual Meeting of the American Society of Mechanical Engineers, Washington, District of Columbia; 1981. p. 1–15.

[28] Brown FT. On weighting functions for the simulation of unsteady turbulent pipe flow. In: Rothe PH, editor. Proceedings of Symposium on Forum on Unsteady Flow. The Winter Annual Meeting of the American Society of Mechanical Engineers, New Orleans, Louisiana, vol. 15.; 1984. p. 26–8.

[29] Brown FT, Linney RE. Wave propagation in tubes with turbulent flow. Part II. Experimental results. In: Franke ME, Drzewiecki TM, editors. Proceedings of Symposium on Fluid Transmission Line Dynamics. The Winter Annual Meeting of

the American Society of Mechanical Engineers, Washington, District of Columbia; 1981. p. 17–32.

[30] Vardy AE, Brown JMB. Transient, turbulent, smooth pipe friction. J Hydraul Res 1995;33(4):435–56.

[31] Shu J-J. A finite element model and electronic analogue of pipeline pressure transients with frequency-dependent friction. Trans ASME, J Fluids Engng 2003;125(1):194–9.

[32] Dukler AE, Ill MW, Cleveland RG. Frictional pressure drop in two-phase flow. Part A. Comparison of existing correlations for pressure loss and holdup. AIChE J 1964;10(1):38–43.

[33] Dukler AE, Ill MW, Cleveland RG. Frictional pressure drop in two-phase flow. Part B. An approach through similarity analysis. AIChE J 1964;10(1):44–51.

[34] Sanada K, Kitagawa A, Takenaka T. A study on analytical methods by classification of column separations in a water pipeline. Trans Jpn Soc Mech Engnr, Ser B 1990;56(523):585–93. In Japanese.

[35] Kephart JT, Davis K. Pressure surges following water-column separation. Trans ASME, J Basic Engng 1961;83:456–60.

[36] Lee IY, Kitagawa A, Takenaka T. On the transient behavior of oil flow under negative pressure. Bull JSME 1985;28(240):1097–104.

[37] Safwat HH, van Den Polder J. Experimental and analytic data correlation study of water column separation. Trans ASME, J Fluids Engng 1973;95:91–7.

[38] Yamaguchi K, Ichikawa T. The transient characteristics of oil pipelines with column separation (some characteristics in pressure histories). Trans Jpn Soc Mech Engnr, Ser B 1985;51(462):536. in Japanese.

[39] Brown RJ. Water-column separation at two pumping plants. Trans ASME, J Basic Engng 1968;90:521–31.

[40] Weyler ME, Streeter VL, Larsen PS. An investigation of the effect of cavitation bubbles on the momentum loss in transient pipe flow. Trans ASME, J Basic Engng 1971;93:1–10.

List of Tables

List of Figures

i	1	2	3	4	5	6	7	8	9	10
n_i	2.63744×10^1	7.28033×10^1	1.87424×10^2	5.36626×10^2	1.57060×10^3	4.61813×10^3	1.36011×10^4	4.00825×10^4	1.18153×10^5	3.48316×10^5
m_i	1.0	1.16725	2.20064	3.92861	6.78788	1.16761×10^1	2.00612×10^1	3.44541×10^1	5.91642×10^1	1.01590×10^2
τ_{m_i}	6.2×10^{-2}	2.8×10^{-2}	9.9×10^{-3}	3.3×10^{-3}	1.1×10^{-3}	3.6×10^{-4}	1.2×10^{-4}	4.1×10^{-5}	1.4×10^{-5}	4.7×10^{-6}

Table 1

	Upstream type	Midstream type	Downstream type
Time tolerance (s)	13.5	3.0	5.0
Upstream pressure (bar)	5.49164	5.58971	4.90325
Downstream pressure (bar)	0.98065	0.98065	0.98065
Initial velocity (m/s)	1.5	1.5	1.45
Radius, r_0 (mm)	7.6		
Length, L (km)	0.2		
Liquid density, ρ_l (kg/m^3)	1000		
Vapour density, ρ_v (kg/m^3)	0.8		
Acoustic velocity, c_0 (m/s)	820		
Vapour pressure, p_v (bar)	0.023		
Liquid viscosity, μ_l (cP)	1.0		
Vapour viscosity, μ_v (cP)	0.0087		

Table 2

Fig. 1

Fig. 2

Upstream
tank

Downstream
tank

(a) Upstream type
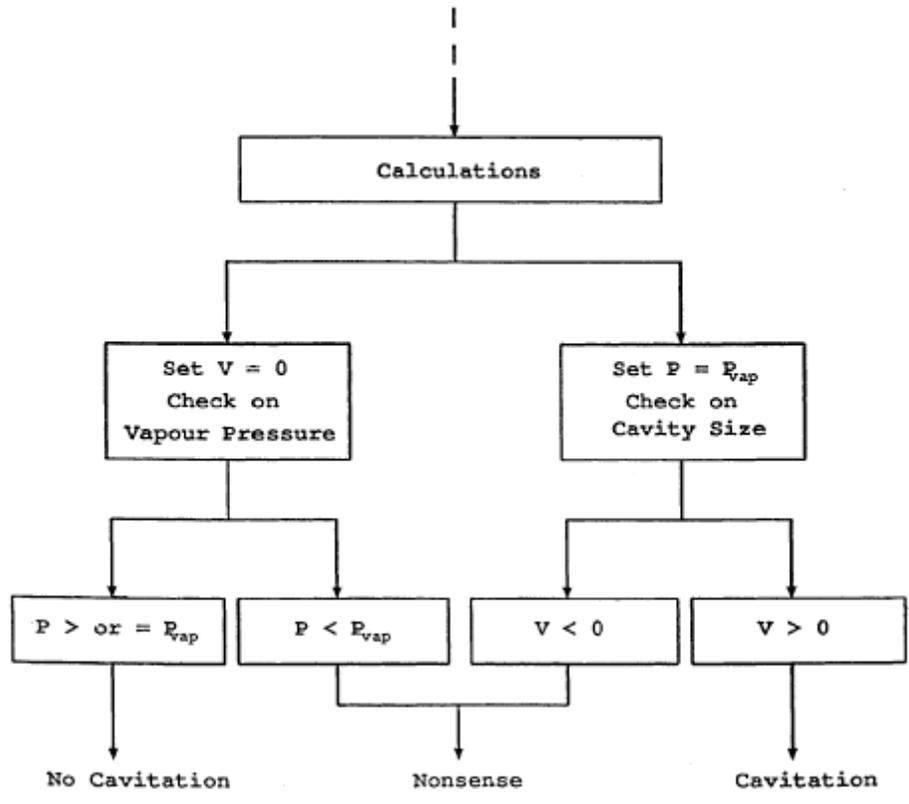
(b) Midstream type

(c) Downstream type

▶ : Cavitation

⟶ : Cause of fluid transients

Fig. 3

Fig. 4

Fig. 5